Atmos. Chem. Phys., 24, 8519–8527, 2024
https://doi.org/10.5194/acp-24-8519-2024

Atmospheric Chemistry and Physics
Open Access
EGU

First observations of the transient luminous event effect on ionospheric Schumann resonance, based on the China Seismo-Electromagnetic Satellite

Shican Qiu[1], Zhe Wang[1], Gaopeng Lu[2], Zeren Zhima[3], Willie Soon[4,5], Victor Manuel Velasco Herrera[6], and Peng Ju[1]

[1]Department of Geophysics, College of Geology Engineering and Geomatics, Chang'an University, Xi'an, 710054, China
[2]Key Laboratory of Geospace Environment, Chinese Academy of Sciences, University of Science and Technology of China, Hefei, 230026, China
[3]China National Institute of Natural Hazards, Ministry of Emergency Management of the PRC, Beijing, 100085, China
[4]Center for Environmental Research and Earth Sciences (CERES), Salem, MA 01970, USA
[5]Institute of Earth Physics and Space Science (ELKH EPSS), Sopron, 9400, Hungary
[6]Instituto de Geofísica, Universidad Nacional Autónoma de México, Mexico City, 04510, Mexico

Correspondence: Shican Qiu (scq@ustc.edu.cn)

Received: 6 February 2024 – Discussion started: 8 February 2024
Revised: 30 April 2024 – Accepted: 31 May 2024 – Published: 31 July 2024

Abstract. In this study, we focus on the interactions and interrelated effects among the transient luminous events (TLEs) recorded at the Luoding ground station (22.76° N, 111.57° E), the lightning activities observed by the World Wide Lightning Location Network, and the ionospheric electric field deduced from the China Seismo-Electromagnetic Satellite (CSES). The results show that on 25 September 2021, the signal-to-noise ratio of the Schumann resonance at the first mode of 6.5 Hz and the second mode of 13 Hz dropped below 2.5 during the TLEs. A significant enhancement in the energy in extremely low frequencies (ELFs) occurred, and the power spectral density increased substantially. Distinct lightning whistler waves were found in the very low frequency (VLF) band, further indicating that the energy could possibly have been excited by the lightning. Our results suggest that the observations of the electric field from the satellite could possibly be utilised to monitor the lower-atmospheric lightning and its impact on the space environment.

1 Introduction

The region from the Earth's ground surface to the ionosphere can be regarded as a spherical resonator with the dielectric atmosphere between the electrically conducting layers (Füllekrug and Fraser-Smith, 1996; Schumann, 1952; Surkov et al., 2013). There are diverse electromagnetic activities in the insulated medium, such as lightning, radioactive particle-induced ionisation, ion annihilation, geomagnetic storms, substorms and cosmic ray input, and electromagnetic waves generated in wide-frequency bands (Füllekrug and Fraser-Smith, 2011; Rycroft et al., 2000; Schumann, 1952). The electromagnetic wave is reflected when it propagates upward into the highly conductive ionosphere, and finally the wave is trapped between the surface and the ionosphere (Füllekrug and Fraser-Smith, 2011; Schumann, 1952). In particular, lightning activity provides the most important source of electromagnetic field energy (Füllekrug and Fraser-Smith, 2011; Rycroft et al., 2000; Willett et al., 1990). The energy generated from lightning is balanced by the energy lost during the propagation process, moderated and maintained under a stable intensity (Füllekrug and Fraser-Smith, 2011). In the resonator cavity, some ultra-low-frequency (ULF) electromagnetic waves can be consistent with the initial phase af-

ter propagating around the Earth for one cycle (Schumann, 1952). These kinds of waves, with frequencies of 7.8, 14, and 20 Hz, can resonate with the phase of the initial wave, that is, the Schumann resonance (SR; Balser and Wagner, 1962; Sátori et al., 2013; Schumann, 1952). Because of the existence of SR, some bands of atmospheric electric field energy will show peaks (e.g. the SR frequency) and valleys (e.g. the non-SR frequency) in the spectral graph (Balser and Wagner, 1962; Galejs, 1970; Sátori et al., 2013; Simões et al., 2011). In 1962, the frequencies of SR were deduced for the first time: $\omega_1 = 7.8$, $\omega_2 = 14.1$, $\omega_3 = 20.1$, and $\omega_4 = 26.6$ Hz (Balser and Wagner, 1962). With more and more SR monitoring stations around the world, the global SR distribution has been obtained (Ouyang et al., 2015; Sátori et al., 2013; Zhou et al., 2013). In 2011, observations from the Communication/Navigation Outage Forecast System (C/NOFS) satellite showed that the electric field energy of the ionospheric F layer increased in some bands, rather consistent with the surface SR mode (Simões et al., 2011). Further, theoretical calculations suggested that the SR can penetrate to the bottom of the ionosphere (Simões et al., 2011; Surkov et al., 2013). Subsequently, the ionospheric SR phenomenon, with an energy of $0.5\,\mu V\,m^{-1}\,Hz^{-1/2}$, was observed by the Chibis-M satellite, and the results proved the existence of F layer SR at low and middle latitudes (Dudkin et al., 2014; Simões et al., 2011; Surkov et al., 2013). These results indicated that SR in the ionosphere could also be provided by the energy rooted in the near-surface atmosphere.

On the other hand, transient luminous events (TLEs) are intense electromagnetic activities occurring in the middle atmosphere, usually generated by tropospheric lightning located below the TLEs (Boccippio et al., 1995; Franz et al., 1990). The TLEs have been determined to exist and have manifested dozens of kilometres above the lightning source regions, requiring strong thunderstorms to energise the electromagnetic waves (Boccippio et al., 1995; Franz et al., 1990; Sentman et al., 1995). TLEs are usually classified into six types according to their shapes and colours: sprites (Mende et al., 1995; Sentman et al., 1995), elves (Fukunishi et al., 1996), blue jets (Wescott et al., 1995), blue starters (Wescott et al., 1996), gigantic jets (Pasko et al., 2002), and halos (Stenbaek-Nielsen et al., 2000). The mechanism of sprites and elves involves the electromagnetic field heating the particles at the bottom of the ionosphere, which will thus provide feedback of a huge amount of energy through differential potentials (Boccippio et al., 1995; Mende et al., 1995; Sentman et al., 1995). TLEs have indeed been found to be closely related to atmospheric and ionospheric electromagnetic activities (Bösinger et al., 2006; Sátori et al., 2013; Shalimov and Bösinger, 2011). For example, the spectral structure of the surface SR has been studied through the sprite Q burst, the electrical impulses generated during TLEs have been analysed, and the ionospheric Alfvén wave resonances excited by jets have been monitored (Bösinger et al., 2006; Füllekrug et al., 1998; Guha et al., 2017). Alfvén waves are thought to be controlled by global lightning activity, which affects the magnetic field in the ionospheric region (Bösinger et al., 2002; Surkov et al., 2013).

In addition, whistler waves can also be generated during lightning events and transmitted into the ionosphere (Bayupati et al., 2012; Carpenter and Anderson, 1992; Holzworth et al., 1999; Storey, 1953). In the 1990s, with the launch of electromagnetic satellites, lightning whistlers were observed in the ionosphere, confirming that large amounts of energy can be coupled to the F layer and even penetrate into the ionosphere (Bayupati et al., 2012; Carpenter and Anderson, 1992; Holzworth et al., 1999). A whistler wave can generally be recognised by a falling frequency (Bernard, 1973; Carpenter and Anderson, 1992; Helliwell, 1965; Helliwell and Pytte, 1966). Intelligent algorithms can now be applied to filter whistler waves from satellite data and locate the lightning source regions (Dharma et al., 2014; Lichtenberger et al., 2008).

Therefore, TLEs can be used as an important carrier or tracer to study the structural coupling of atmospheric layers. However, there are still many gaps in research on TLEs because it is relatively difficult to observe them. On the other hand, the ionospheric SR energy comes from the surface and is closely related to the space environment. In this study, we utilise the latest data on ionospheric electric field from the China Seismo-Electromagnetic Satellite (CSES) for the first time to study the relationship between TLEs and ionospheric SR through the methods of the signal-to-noise ratio (SNR) and the power spectral density (PSD).

2 Materials and methods

The TLEs captured and observed by the Luoding monitoring station will be analysed. The electromagnetic field data come from the CSES satellite, orbiting at an altitude of 500 km around the F layer of the ionosphere (Diego et al., 2020). It is designed to adopt a 5 d revisit cycle, with a daily progression of 500 km eastward (Diego et al., 2020). The data length of each sampling point in the extremely low frequency (ELF) band is 256, and the sampling frequency is about 100 Hz with an interval of 8 ms (Diego et al., 2020). Each sample point of the very low frequency (VLF) band has a length of 2048, a frequency of 12 kHz, and an interval of 80 µs (Diego et al., 2020). The lightning observations are provided by the World Wide Lightning Location Network (WWLLN), recording the time, latitude, and longitude of the lightning (Jacobson et al., 2006). In order to obtain the corresponding ionospheric SR characteristics, the electric field from the CSES satellite data with the closest orbit is utilised.

The methods for data processing are the signal-to-noise ratio (SNR) and the power spectral density (PSD). The SNR is a method proposed to study the field perturbations (Molchanov et al., 2006). Its main principle is to measure the amplitude of the perturbation through energy from a specific

band relative to the chosen or reference bands. The calculation of SNR is given as

$$\mathrm{SNR} = \frac{2A(f_0)}{A(f_-) + A(f_+)}, \quad (1)$$

where $A(f_0)$ is the energy corresponding to the signal f_0, $A(f_-)$ is the noise energy whose band is lower than the SR signal, and $A(f_+)$ is the noise energy with a band higher than the SR signal. Then we can set the peak frequency of SR as the signal f_0, the field frequency lower than SR as f_-, and larger than SR as f_+.

The principle of the PSD method is spectrum analysis from the Fourier transform (Bracewell and Kahn, 1966; Bracewell, 1989). The frequency domain information of each sampling point is calculated to obtain the spectrum. Then, the frequency domain data are arranged in the order of time or space to draw a three-dimensional PSD map. The calculation of the Fourier transform is given as

$$F(s) = \int_{-\infty}^{+\infty} f(x) e^{-i2\pi xs} \mathrm{d}x, \quad (2)$$

where $F(s)$ represents the frequency domain, and $f(x)$ is the time domain.

3 Observations and discussion

The TLEs captured by the Luoding station in 2021 are shown as the orange stars in Fig. 2. The TLEs were mainly concentrated in May to September, consistent with the local thunderstorm season. We focus on the case of 25 September 2021 to study the ionospheric SR anomalies during the TLEs. A total of 36 TLEs were photographed between 16:00 and 20:00 UT. Some of the more prominent TLEs are shown in Fig. 1a–f, taken at 17:59, 18:38, 18:53, 19:01, 19:49, and 20:07 UT, respectively. All of the TLEs shown in Fig. 1 are classified as red sprites.

On the other hand, the observations from WWLLN exhibited huge thunderstorm activities developing near Hainan Island. The lightning was mainly concentrated in the range of 18–22° N, 110–113° E, 200 km southeast of Luoding station. Around 15:00 UT, the lightning appeared and continued until 22:00 UT. Therefore, the duration of the thunderstorm included the main time when the TLEs occurred over Luoding. The pink dots in Fig. 2b and e show the lightning mainly as it occurred within the 17:00 to 20:00 UT time window.

Comparing the CSES orbit time with the occurrence of TLEs, we selected the nighttime side data of orbit no. 20239 for analysis. The CSES orbital position passed near Luoding station at around 18:33 UT, located on the west side with a horizontal distance of about 200 km. Data points were selected for the background data from September to October around the same orbital positions, i.e. the repeat of the satellite's orbit around Luoding after every 5 d cycle. The appropriate CSES satellite orbits were found on 20 September and 15 October. No TLEs were captured on 15 October. On 20 September, TLEs were only photographed during the 13:00–15:00 UT period, with no TLEs appearing when CSES travelled over Luoding station at 18:00 UT. The lightning on 20 September and 15 October is also shown in Fig. 2a and c. It can be seen and confirmed that there were no large-scale thunderstorm areas on 20 September and 15 October.

Taking the SR as the signal and the non-SR as the noise, the variations in SNR with latitude can be calculated. Through evaluation and analysis, the first mode of SR is assigned to be 6.5 Hz, while 3 and 8 Hz are adopted accordingly as the upper and lower bands. The second mode of SR is assigned to be 13 Hz, with 10 and 16 Hz as the upper and lower noise bands, respectively. According to the SNR calculation method from Eq. (1), the background SNR is shown is Fig. 2a, c, d, and f. In comparison, the SNR for CSES orbit no. 20239 is given in Fig. 2b and e. The red, green, and blue circles indicate SNR > 5, $2.5 <$ SNR < 5, and SNR < 2.5, respectively. Figure 2a, c, d, and f demonstrate that the background SR has SNR above 2.5, with many of the sampling points even above 5 when there is no disturbance. Figure 2b and e show the SR's first and second modes for the no. 20239 orbit, respectively. The decrease in SNR is mainly concentrated in the area between 10–22° N, shown as the blue circles. This region is close to the lightning area that developed near Hainan Island, with the point at 18° N located just over the thunderstorms. Accompanied by the occurrence of a large amount of lightning and a number of TLEs, the SNR is significantly reduced to below 2.5, with a first mode of 1.9 and second mode of 1.2.

Figure 3 shows the energy distribution of all bands in the range of 1–20 Hz on the 3 days, exhibiting the energy variation with frequency and latitude, i.e. the PSD. It includes the first mode of the SR at 6.5 Hz and the second mode at 13 Hz. Figure 3a and c represent the PSDs on 20 September and 15 October, respectively, when both the lightning activities and TLEs were weak. In Fig. 3a and c, the electric field energy is concentrated in the two bands of SR, which is much higher than that of the non-SR bands. The peak frequency of SR remains stable, and the overall variation does not exceed 0.5 Hz. However, when the TLEs appear, the PSD in Fig. 3b exhibits obvious perturbations. The electric field energy recorded by CSES orbit no. 20239 is not concentrated in the SR band but is distributed and spread more broadly in the band from 1 to 20 Hz. Within the 10–22° N region on 25 September, the PSD is significantly enhanced, especially in the non-SR bands. In the 23–30° N region, the PSD still maintains two distinct SR modes, which is consistent with the background as shown in Fig. 3a and c. The peak field strength of the first and second SR modes is about $0.5\,\mu\mathrm{V\,m^{-1}\,Hz^{-1/2}}$, which is consistent with the Chibis-M satellite data (Dudkin et al., 2014; Simões et al., 2011). It was found that the enhanced region in Fig. 3b is consistent with the region of decreasing SNR in Fig. 2b and e. Therefore, we believe that during the no. 20239 orbit, the ionospheric

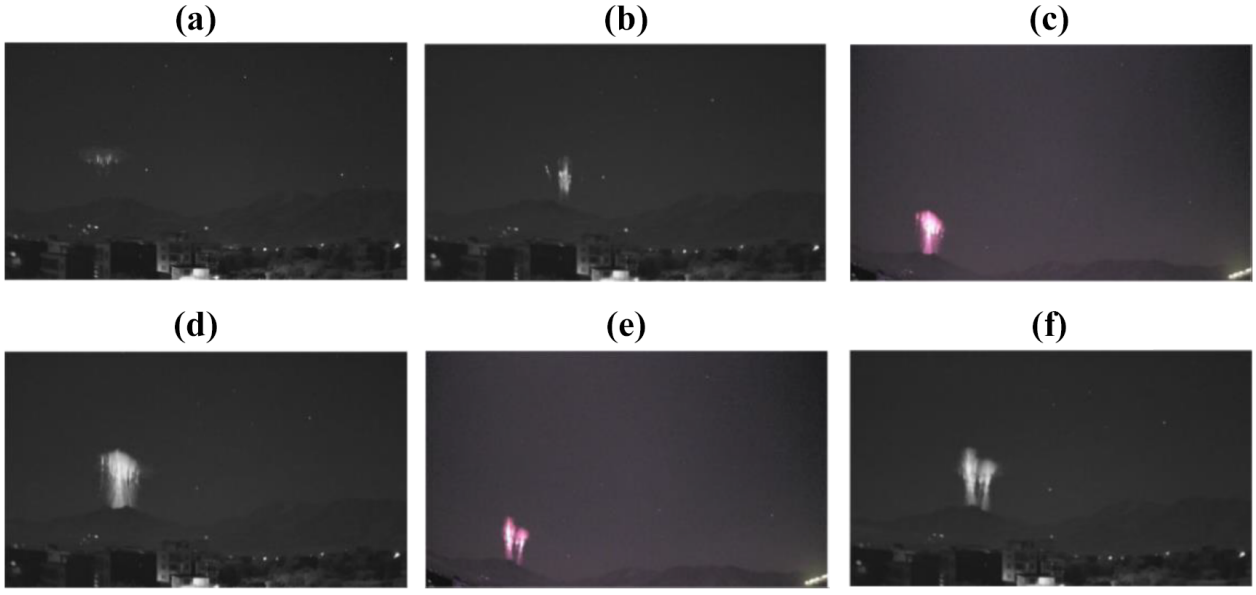

Figure 1. The transient luminous events (TLEs) captured around the Luoding station on 25 September 2021 at **(a)** 17:59, **(b)** 18:38, **(c)** 18:53, **(d)** 19:01, **(e)** 19:49, and **(f)** 20:07 UT.

F layer in the 10–22° N region underwent significant disturbances due to the combined action of both lightning and TLE activities.

We can further verify that the low-Earth-orbiting satellite can record the electromagnetic energy from coupled lightning and TLEs to the top of the ionosphere. Figure 4 shows the lightning whistler waves recorded by the electric field meter (panel a) and the magnetometer (panel b) during the no. 20239 orbit around 18:31 UT, when the CSES satellite was located at 16.5° N. The whistler waves recorded by CSES range from 16–20° N, which coincides with the distribution area of the lightning activities. The whistler wave durations are within 1–2 s, and the frequencies are generally in the range of 3–10 kHz, which is consistent with a typical whistler wave phenomenon (Bayupati et al., 2012; Carpenter and Anderson, 1992; Holzworth et al., 1999). As the high-frequency whistler wave has a higher group velocity and is the first to be received, it shows the characteristic falling frequency in the PSD. These whistler wave signals indicate that the electromagnetic field generated by lightning and TLEs can be superimposed onto the ionospheric electric field, resulting in an increase in the energy of the electric field in a certain band.

Furthermore, we analyse the latitude-dependent energy in each band of the ELF, as shown in Fig. 5. Among them, 18.07 Hz is the third mode of SR with weaker energy (shown by the red line), 12.69 Hz is the second mode of SR (blue), and 6.34 Hz is the first mode (green). The solid line represents the measured electric field during CSES orbit no. 20239, the dashed line shows the observation on 20 September, and the dotted line denotes the electric field on 15 October. It was found that in the 10–22° N region, the energy in each band of the no. 20239 orbit was much stronger, while the energy during the 3 days was almost the same in the region of 23–30° N. We calculated that the increase in the energy in each band within the 10–22° N region is 300 % at 6.34 Hz, 270 % at 12.69 Hz, and 130 % at 18.07 Hz. The energy of the first mode (i.e. 6.34 Hz) and the second mode (i.e. 12.69 Hz) of the SR is enhanced significantly, while the energy of the faint third mode also increases noticeably. Therefore, the decrease in SNR during the TLEs could reasonably have been caused by the energy increase in the non-SR band.

The electric field energy of the three bands has a maximum enhancement near 17.5° N, very close to the range of lightning activity in Fig. 3b. At the same time, the electromagnetic field of the VLF band in this area also records the presence of whistler waves (Fig. 4). Therefore, we believe that the electric field disturbance of the no. 20239 orbit was caused by lightning and TLE activity. The results show that when lightning and TLEs occur, the electric field with lower frequency is more likely to penetrate into the high-conductance region of the ionosphere. This energy causes the ionospheric electric field to be disturbed, the energy of each band of ELF increases, and the SNR of SR decreases. That is, the electric field generated during lightning and TLEs superimposes energy onto each band of the ionosphere, just as whistler wave energy superimposes onto the VLF band.

In order to make the new results more credible, we further examine and study the variation in the geomagnetic disturbance storm time (Dst) index for September 2021 and the large-scale geological activities. We found that there was no strong geomagnetic storm around September 2021, nor was any prominent geological activity obvious near Luoding. In order to exclude the influence of other factors, we

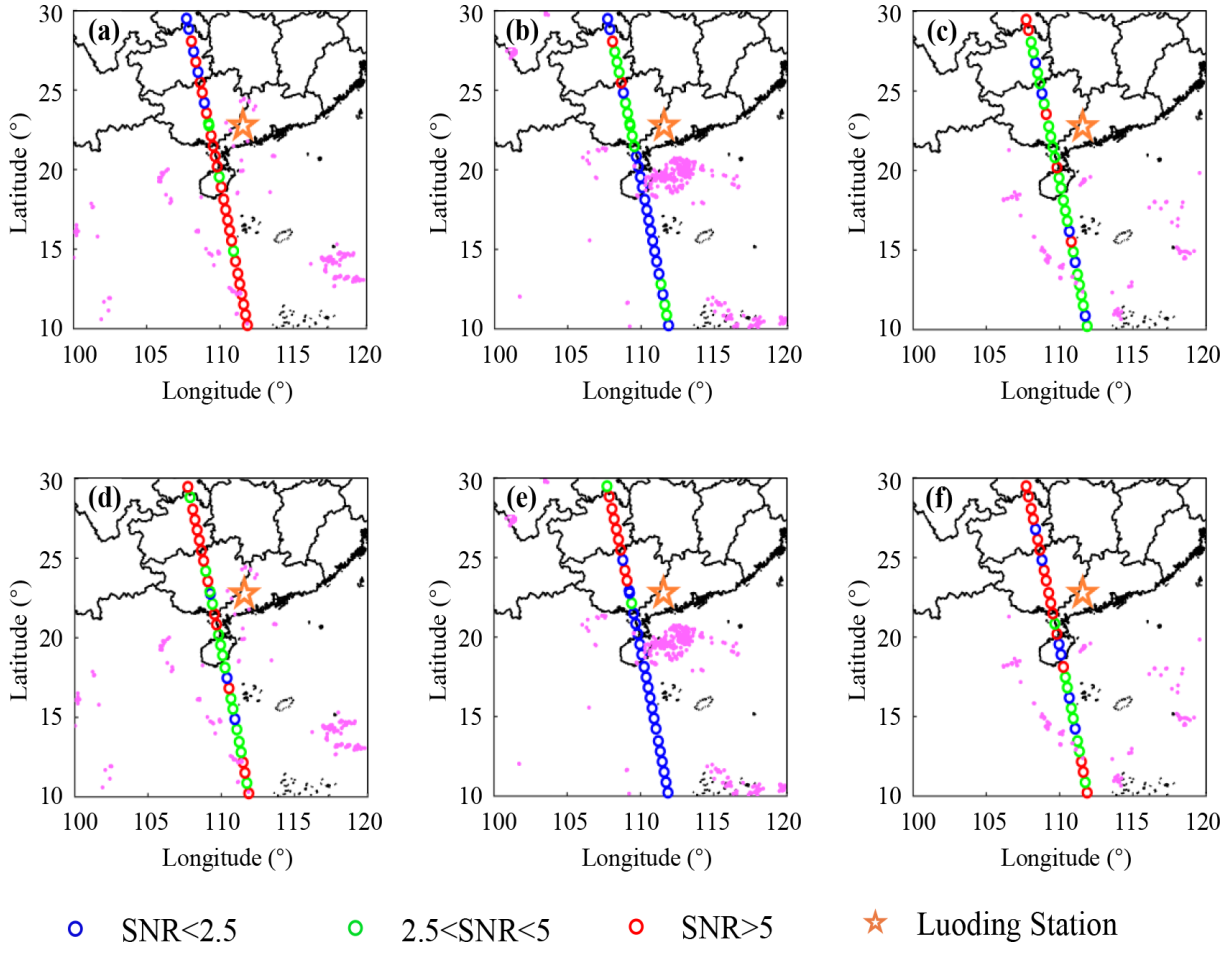

Figure 2. The signal-to-noise ratio (SNR) for the Schumann resonance (SR) of the ionospheric electric field and the distributions of the lightning. The red, green, and blue circles indicate the SNR > 5, 2.5 < SNR < 5, and SNR < 2.5, respectively. The pink dots show the lightning locations. The orange star represents Luoding station. **(a)** The SNR of the first mode on 20 September 2021 and the lightning from 17:00 to 20:00 UT. **(b)** The SNR in the first mode of the no. 20239 orbit of CSES on 25 September 2021 and lightning distributions. **(c)** The SNR of the first mode on 15 October 2021 and lightning distributions. **(d)** The SNR of the second mode on 20 September 2021. **(e)** The SNR of the second mode of the no. 20239 orbit. **(f)** The SNR of the second mode on 15 October 2021.

examined the possible influence of solar activity and high-energy proton events. The data showed that the solar activity was relatively calm during these days, and there were also no high-energy particle events. Therefore, based on the observations, we conclude that the ionospheric anomalies on 25 September 2021 could possibly have been controlled by the two factors of lightning and TLEs. The TLEs captured were all red sprites, whose formation mechanism is an electromagnetic pulse transferring energy to the bottom of the ionosphere. Then the TLEs may cause dramatic changes in the ionospheric particles and obvious disturbances in electromagnetic field energy. However, lightning activities also produce Alfvén waves, which are close to the two modes of SR and may interfere with the ionospheric SR (Beggan and Musur, 2018; Dudkin et al., 2014). Therefore, we further analysed the time–frequency characteristics of the interference patterns between Alfvén waves and the Schumann resonance, comparing with the electric field disturbance. The interference pattern generally manifests as a specific fingerprint shape. However, the SR anomaly observed in Fig. 3 is quite different from these particular interference characteristics. Thus, we believe that this anomaly is not caused by Alfvén waves.

The lightning whistler wave suggests that the electromagnetic energy will be transported to the altitude range of the satellite orbit. The specific coupling process could be proposed as follows: the lightning and TLEs generate electromagnetic waves in multiple bands; in the process of upward coupling, electric fields in many bands can transmit energy to the ionosphere; and when these electromagnetic waves penetrate into the ionosphere, energy can be coupled to the satellite orbit around the F layer of the ionosphere. Since the electromagnetic field has been generated in both the SR band and non-SR band, the energy increase in multiple bands is ob-

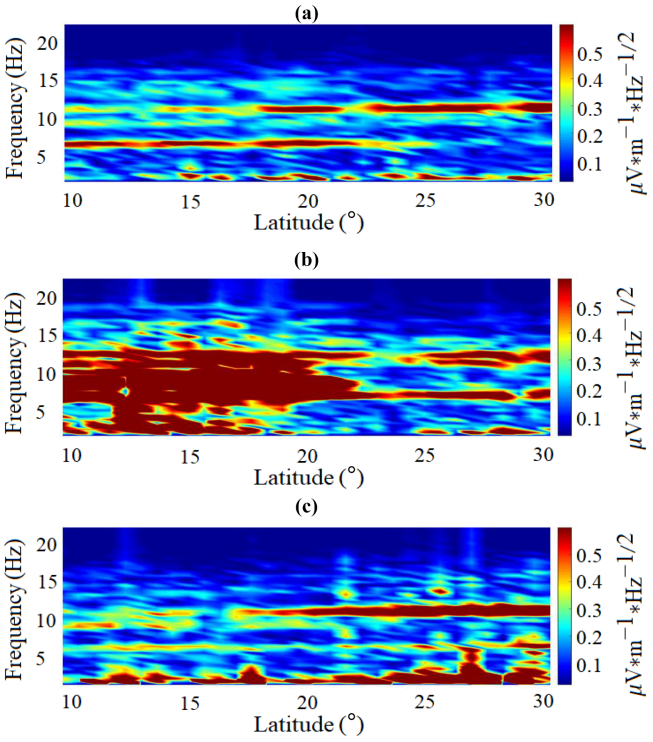

Figure 3. The power spectral density (PSD) of the ionospheric electric field SR. **(a)** The electric field PSD on 20 September 2021. **(b)** The electric field PSD of CSES orbit no. 20239 on 25 September. **(c)** The electric field PSD on 15 October. In **(a)** and **(c)**, the PSD has two obvious peak lines at 6.5 and 13 Hz as the first and second modes of the SR, respectively.

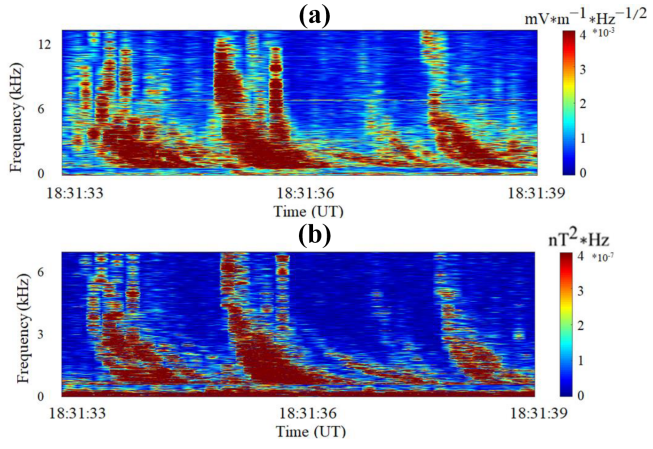

Figure 4. The lightning whistler waves in obvious falling frequency displayed during orbit no. 20239, observed at 18:31:36 UT at 16.6° N. **(a)** The lightning whistler waves measured by the electric field meter. **(b)** The power spectral density of the lightning-generated whistler waves observed by the magnetometer.

served by the CSES satellite. In the ionospheric background, the SR energy is supplied by the lower boundary near the surface region, manifested as the peak energy in specific bands

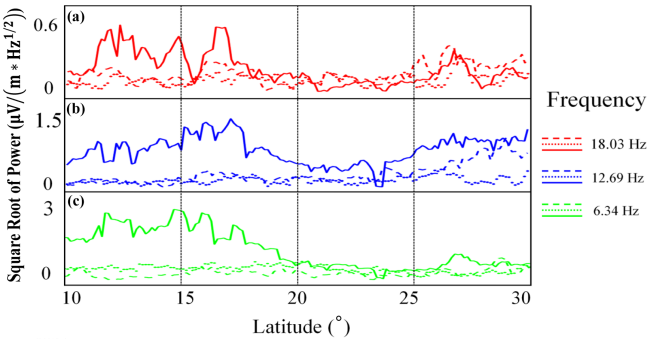

Figure 5. The energy variations in the electric field in each ELF band, from CSES orbit no. 20239. The lines in red, blue, and green colours represent the energy intensity at 18.07, 12.69, and 6.34 Hz, respectively. The solid line is the measured electric field during orbit no. 20239 on 25 September. The dashed line indicates the electric field on 20 September, and the dotted line denotes the electric field on 15 October.

(Fig. 3a and c). When the perturbation of the electromagnetic field from the lightning activities and TLEs is superimposed on the ionosphere, the energy of each band will increase obviously in the PSD (Figs. 3b and 5). The energy proportion of SR will decrease, leading to the decrease in the SNR. Since the energy attenuation in the low-frequency electric field is small, for the ELF band, the stronger energy of the electric field is, the stronger the SR perturbation will be. In the VLF band, the electric field meter and magnetometer recorded the lightning whistler waves, while in the ELF band, the electric field energy showed an anomalous increase. Besides, the remaining 13 cases of TLEs documented near the Luoding station were also analysed, and 6 of those cases appeared near Luoding station close to 18:30 UT. In two cases, SR data were recorded by CSES, which exhibited similar perturbations. Therefore, this perturbation may be widespread during TLE activity.

4 Conclusions

In this research, the latest ionospheric electric field data from the CSES satellite are utilised for the first time to the study the disturbance of ionospheric SR during lightning and TLE events. The results show that the disturbances of the ionospheric electric field can be coupled upward to the CSES orbital altitude and lead to strong SR perturbations. The electric field variations can be represented and studied in terms of PSD and SNR diagnostic metrics. The disturbance of SR is mainly in the ELF band, while the whistler wave is in the VLF band. Our results suggest the existence of a coupling to the ionospheric F layer via lightning and TLEs.

The conclusions are given as follows:

1. A huge lightning and TLE event co-occurred on 25 September 2021, penetrated to the bottom of the

ionosphere, and caused electric field disturbance in the upper satellite orbit region. During the lightning activity, the horizontal range of this disturbance can reach hundreds of kilometres.

2. The lightning activities and TLEs increased the PSD energy of the ionospheric electric field and reduced the signal-to-noise ratio of the first and second modes of Schumann resonance. Comparing the Alfvén wave with the SR interference phenomenon, we believe that it is likely that this disturbance is indeed caused by the electric field originating from lightning instead of from the Alfvén wave.

3. When the SR disturbance occurred in the ELF band of the electric field, the whistler wave signal was detected in the VLF band. The whistler wave indicates that the electric field energy generated by the lightning and TLEs can cause disturbances up to altitudes as high as the CSES satellite orbit.

Data availability. The dataset of transient luminous events over high-impact thunderstorm systems comes from the National Space Science Data Center, https://doi.org/10.12176/01.05.00070-V01 (University of Science and Technology of China, 2021a). The coordinated observations of transient luminous events data are available from the National Space Science Data Center, https://doi.org/10.12176/01.05.00069-V01 (University of Science and Technology of China, 2021b). The ionosphere data of the China Seismo-Electromagnetic Satellite (CSES) can be downloaded from the database after registering to select the specific kind of data (https://leos.ac.cn, CSES, 2019) after registering to select the specific kind of data. The lightning location and power data, with updates every 10 min, are available from the World Wide Lightning Location Network from the University of Washington (http://wwlln.net/ WWLLN, 2024).

Author contributions. SQ conceived this study and wrote this paper. ZW performed data analysis and prepared the figures. GL added some material about transient luminous events and lightning strikes. ZZ supplied some data from the China Seismo-Electromagnetic Satellite. WS was in charge of the organisation and English polishing of the whole paper. VMVH contributed to the data processing and analyses. PJ added some material to the discussion.

Competing interests. The contact author has declared that none of the authors has any competing interests.

Disclaimer. Publisher's note: Copernicus Publications remains neutral with regard to jurisdictional claims made in the text, published maps, institutional affiliations, or any other geographical representation in this paper. While Copernicus Publications makes every effort to include appropriate place names, the final responsibility lies with the authors.

Acknowledgements. This work was supported by the Fundamental Research Funds for the Central Universities, CHD (grant no. 300102263205), and the West Light Cross-Disciplinary Innovation team of the Chinese Academy of Sciences (grant no. E1294301). This work has made use of the data from the China Seismo-Electromagnetic Satellite (CSES) mission, a project funded by the China National Space Administration (CNSA) and the China Earthquake Administration (CEA). We acknowledge the data resources from the National Space Science Data Center, National Science and Technology Infrastructure of China. We thank the World Wide Lightning Location Network (WWLLN) for the use of their data.

Financial support. This research has been supported by the Fundamental Research Funds for the Central Universities (grant nos. 300102263205 and 300102264916).

Review statement. This paper was edited by John Plane and reviewed by two anonymous referees.

References

Balser, M. and Wagner, C. A.: On frequency variations of the Earth-ionosphere cavity modes, J. Geophys. Res., 67, 4081–4083, https://doi.org/10.1029/JZ067i010p04081, 1962.

Bayupati, I. P. A., Kasahara, Y., and Goto, Y.: Study of dispersion of lightning whistlers observed by Akebono satellite in the earth's plasmasphere, IEICE T. Commun., 95, 3472–3479, 2012.

Beggan, C. D. and Musur, M.: Observation of ionospheric Alfvén resonances at 1–30 Hz and their superposition with the Schumann resonances, J. Geophys. Res.-Space, 123, 4202–4214, https://doi.org/10.1029/2018JA025264, 2018.

Bernard, L. C.: A new nose extension method for whistlers, J. Atmos. Terr. Phys., 35, 871–880, https://doi.org/10.1016/0021-9169(73)90069-X, 1973.

Boccippio, D. J., Williams, E. R., Heckman, S. J., Lyons, W. A., Baker, I. T., and Boldi, R.: Sprites, ELF transients, and positive ground strokes, Science, 269, 1088–1091, https://doi.org/10.1126/science.269.5227.1088, 1995.

Bösinger, T., Haldoupis, C., Belyaev, P. P., Yakunin, M. N., Semenova, N. V., Demekhov, A. G., and Angelopoulos, V.: Spectral properties of the ionospheric Alfvén resonator observed at a low-latitude station ($L = 1.3$), J. Geophys. Res.-Space, 107, SIA 4-1–SIA 4-9, https://doi.org/10.1029/2001JA005076, 2002.

Bösinger, T., Mika, A., Shalimov, S. L., Haldoupis, C., and Neubert, T.: Is there a unique signature in the ULF response to sprite-associated lightning flashes?, J. Geophys. Res.-Space, 111, A10310, https://doi.org/10.1029/2006JA011887, 2006.

Bracewell, R. and Kahn, P. B.: The Fourier Transform and Its Applications, Am. J. Phys., 34, 712–712, https://doi.org/10.1119/1.1973431, 1966.

Bracewell, R. N.: The fourier transform, Sci. Am., 260, 86–95, https://doi.org/10.1038/scientificamerican0689-86, 1989.

Carpenter, D. L. and Anderson, R. R.: An ISEE/whistler model of equatorial electron density in the magneto-

sphere, J. Geophys. Res.-Space, 97, 1097–1108, 1992, https://doi.org/10.1029/91JA01548, 1992.

CSES: Center for Space Information Research, China Seismo-Electromagnetic Satellite (CSES), https://leos.ac.cn (last access: 28 October 2023), 2019.

Dharma, K. S., Bayupati, I. P. A., and Buana, P. W.: Automatic lightning whistler detection using connectd component method, Journal of Theoretical and Applied Information Technology, 66, 638–645, 2014.

Diego, P., Huang, J., Piersanti, M., Badoni, D., Zeren, Z., Yan, R., Rebustini, G., Ammendola, R., Candidi, M., Guan, Y. B., Lei, J., Masciantonio, G., Bertello, I., De Santis, C., Ubertini, P., Shen, X., and Picozza, P.: The electric field detector on board the China seismo electromagnetic satellite – In-orbit results and validation, Instruments, 5, 1, https://doi.org/10.3390/instruments5010001, 2020.

Dudkin, D., Pilipenko, V., Korepanov, V., Klimov, S., and Holzworth, R.: Electric field signatures of the IAR and Schumann resonance in the upper ionosphere detected by Chibis-M microsatellite, J. Atmos. Sol.-Terr. Phy., 117, 81–87, https://doi.org/10.1016/j.jastp.2014.05.013, 2014.

Franz, R. C., Nemzek, R. J., and Winckler, J. R.: Television image of a large upward electrical discharge above a thunderstorm system, Science, 249, 48–51, https://doi.org/10.1126/science.249.4964.48, 1990.

Fukunishi, H., Takahashi, Y., Kubota, M., Sakanoi, K., Inan, U. S., and Lyons, W. A.: Elves: Lightning-induced transient luminous events in the lower ionosphere, Geophys. Res. Lett., 23, 2157–2160, https://doi.org/10.1029/96GL01979, 1996.

Füllekrug, M. and Fraser-Smith, A. C.: Further evidence for a global correlation of the Earth-ionosphere cavity resonances, Geophys. Res. Lett., 23, 2773–2776, https://doi.org/10.1029/96GL02612, 1996.

Füllekrug, M. and Fraser-Smith, A. C.: The Earth's electromagnetic environment, Geophys. Res. Lett., 38, L21807, https://doi.org/10.1029/2011GL049572, 2011.

Füllekrug, M., Fraser-Smith, A. C., and Reising, S. C.: Ultra-slow tails of sprite-associated lightning flashes, Geophys. Res. Lett., 25, 3497–3500, https://doi.org/10.1029/98GL02590, 1998.

Galejs, J.: Frequency variations of Schumann resonances, J. Geophys. Res., 75, 3237–3251, https://doi.org/10.1029/JA075i016p03237, 1970.

Guha, A., Williams, E., Boldi, R., Sátori, G., Nagy, T., Bór, J., Montanya, J., and Ortega P.: Aliasing of the Schumann resonance background signal by sprite-associated Q-bursts, J. Atmos. Sol.-Terr. Phy., 165, 25–37, https://doi.org/10.1016/j.jastp.2017.11.003, 2017.

Helliwell, R. A.: Whistlers and related ionospheric phenomena, Stanford University Press, Stanford, America, 349 pp., ISBN 0-486-44572-0, 1965.

Helliwell, R. A. and Pytte, A.: Whistlers and related ionospheric phenomena, Am. J. Phys., 34, 81–81, https://doi.org/10.1119/1.1972800, 1966.

Holzworth, R. H., Winglee, R. M., Barnum, B. H., Li, Y., and Kelley, M. C.: Lightning whistler waves in the high-latitude magnetosphere, J. Geophys. Res.-Space, 104, 17369–17378, https://doi.org/10.1029/1999JA900160, 1999.

Jacobson, A. R., Holzworth, R., Harlin, J., Dowden, R., and Lay, E.: Performance assessment of the world wide lightning location network (WWLLN), using the Los Alamos sferic array (LASA) as ground truth, J. Atmos. Ocean. Tech., 23, 1082–1092, https://doi.org/10.1175/jtech1902.1, 2006.

Lichtenberger, J., Ferencz, C., Bodnár, L., Hamar, D., and Steinbach, P.: Automatic whistler detector and analyzer system: Automatic whistler detector, J. Geophys. Res.-Space, 113, A12201, https://doi.org/10.1029/2008JA013467, 2008.

Mende, S. B., Rairden, R. L., Swenson, G. R., and Lyons, W. A.: Sprite spectra; N_2 1 PG band identification, Geophys. Res. Lett., 22, 2633–2636, https://doi.org/10.1029/95GL02827, 1995.

Molchanov, O., Rozhnoi, A., Solovieva, M., Akentieva, O., Berthelier, J. J., Parrot, M., Lefeuvre, F., Biagi, P. F., Castellana, L., and Hayakawa, M.: Global diagnostics of the ionospheric perturbations related to the seismic activity using the VLF radio signals collected on the DEMETER satellite, Nat. Hazards Earth Syst. Sci., 6, 745–753, https://doi.org/10.5194/nhess-6-745-2006, 2006.

Ouyang, X. Y., Xiao, Z., Hao, Y. Q., and Zhang, D. H.: Variability of Schumann resonance parameters observed at low latitude stations in China, Adv. Space Res., 56, 1389–1399, https://doi.org/10.1016/j.asr.2015.07.006, 2015.

Pasko, V. P., Stanley, M. A., Mathews, J. D., Inan, U. S., and Wood, T. G.: Electrical discharge from a thundercloud top to the lower ionosphere, Nature, 416, 152–154, https://doi.org/10.1038/416152a, 2002.

Rycroft, M. J., Israelsson, S., and Price, C.: The global atmospheric electric circuit, solar activity and climate change, J. Atmos. Sol.-Terr. Phy., 62, 1563–1576, https://doi.org/10.1016/S1364-6826(00)00112-7, 2000.

Sátori, G., Rycroft, M., Bencze, P., Märcz, F., Bór, J., Barta, V., Nagy, T., and Kovács, K.: An Overview of Thunderstorm-Related Research on the Atmospheric Electric Field, Schumann Resonances, Sprites, and the Ionosphere at Sopron, Hungary, Surv. Geophys., 34, 255–292, https://doi.org/10.1007/s10712-013-9222-6, 2013.

Schumann, W. O.: On the free oscillations of a conducting sphere which is surrounded by an air layer and an ionosphere shell, Z. Naturforsch., 7A, 149–154, 1952 (in German).

Shalimov, S. L. and Bösinger, T.: Sprite-Producing Lightning-Ionosphere Coupling and Associated Low-Frequency Phenomena, Space Sci. Rev., 168, 517–531, https://doi.org/10.1007/s11214-011-9812-x, 2011.

Sentman, D. D., Wescott, E. M., Osborne, D. L., Hampton, D. L., and Heavner M. J.: Preliminary results from the Sprites94 Aircraft Campaign: 1. Red sprites, Geophys. Res. Lett., 22, 1205–1208, https://doi.org/10.1029/95GL00583, 1995.

Simões, F., Pfaff, R., and Freudenreich, H.: Satellite observations of Schumann resonances in the Earth's ionosphere, Geophys. Res. Lett., 38, L22101, https://doi.org/10.1029/2011GL049668, 2011.

Stenbaek-Nielsen, H. C., Moudry, D. R., Wescott, E. M., Sentman, D. D., and Sâo Sabbas, F. T.: Sprites and possible mesospheric effects, Geophys. Res. Lett., 27, 3829–3832, https://doi.org/10.1029/2000GL003827, 2000.

Storey, L. R. O.: An investigation of whistling atmospherics, Philos. T. R. Soc. S.-A, 246, 113–141, https://doi.org/10.1098/rsta.1953.0011, 1953.

Surkov, V. V., Nosikova, N. S., Plyasov, A. A., Pilipenko, V. A., and Ignatov, V. N.: Penetration of Schumann resonances into the upper ionosphere, J. Atmos. Sol.-Terr. Phy., 97, 65–74, https://doi.org/10.1016/j.jastp.2013.02.015, 2013.

University of Science and Technology of China: Transient luminous events over high-impact thunderstorm systems 1.0, National Space Science Data Center [data set], 8 October 2021, https://doi.org/10.12176/01.05.00070-V01, 2021a.

University of Science and Technology of China: Coordinated Observations of Transient Luminous Events 1.0, National Space Science Data Center [data set], 27 September 2021, https://doi.org/10.12176/01.05.00069-V01, 2021b.

Wescott, E. M., Sentman, D. D., Osborne, D., Hampton, D., and Heavner, M.: Preliminary results from the Sprites94 Aircraft Campaign: 2. Blue jets, Geophys. Res. Lett., 22, 1209–1212, https://doi.org/10.1029/95GL00582, 1995.

Wescott, E. M., Sentman, D. D., Heavner, M. J., Hampton, D. L., Osborne, D. L., and Vaughan Jr., O. H.: Blue starters: Brief upward discharges from an intense Arkansas thunderstorm, Geophys. Res. Lett., 23, 2153–2156, https://doi.org/10.1029/96GL01969, 1996.

Willett, J. C., Bailey, J. C., Leteinturier, C., and Krider, E. P.: Lightning electromagnetic radiation field spectra in the interval from 0.2 to 20 MHz, J. Geophys. Res.-Atmos., 95, 20367–20387, https://doi.org/10.1029/JD095iD12p20367, 1990.

WWLLN: World Wide Lightning Location Network, WWLLN [data set], http://wwlln.net/ (last access: 28 October 2023), 2024.

Zhou, H., Yu, H., Cao B., and Qiao, X.: Diurnal and seasonal variations in the Schumann resonance parameters observed at Chinese observatories, J. Atmos. Sol.-Terr. Phy., 98, 86–96, https://doi.org/10.1016/j.jastp.2013.03.021, 2013.